

# Cyclic voltammetric investigation of the formation of intermetallic phases at a LiAl electrode in methyl acetate

Y. S. FUNG, H. C. LAI

*Department of Chemistry, University of Hong Kong, Hong Kong*

Received 27 September 1990; revised 2 June 1991

The formation of various Li/Al intermetallic phases at the LiAl electrode in methyl acetate was studied using cyclic voltammetry. The thickness of the  $\alpha$  phase formed initially was estimated using the deposition and stripping method to be 1.1 nm. Repetitive cycling at the  $\alpha$  or  $\beta$  phase potential led to a drastic increase in current over the first ten cycles before reaching a steady state. The formation of the  $\beta$  phase depended critically on the deposition potential and its presence at the electrode surface led to enhanced current in the reverse sweep, increased acceptance of deposited lithium, roughening and development of the area of the electrode upon cycling. The above effects were attributed to the difference in the lattice structure of the  $\beta$  phase as compared to the  $\alpha$  phase, which greatly affected the electrode kinetics upon phase transition. The deposition of the more reactive LiAl alloys at more cathodic potential, namely  $-3.80$  V, led to the formation of a passivating film which was broken down at more cathodic potential when the electrode surface had undergone vigorous chemical reaction with the solvent. Methyl acetoacetate was identified using i.r., n.m.r., u.v. and electrochemical techniques to be the major reaction product and a possible reaction mechanism was proposed.

## 1. Introduction

Due to the wide electrochemical window, low density, low melting point and commercial availability, various organic solvents have been investigated extensively for use as electrochemical solvent media for secondary ambient temperature lithium batteries. Propylene carbonate [1–5],  $\gamma$ -lactone based electrolytes [6], 1,3-dioxolane [7, 8], tetrahydrofuran [9–11], 2-methyltetrahydrofuran [12, 13], methyl acetate [14, 15] and dimethoxyethane [16] have been studied in detail. However, all were found to be reactive towards the lithium anode, thus limiting their use for secondary lithium batteries.

A previous study [17] has shown that a vigorously purified methyl acetate (MA) can provide a promising solvent system as 95% cycling efficiency was obtained with low capacity loss current (0.26% of the plating current) upon cycling with the LiAl electrode in MA. Water and other organic impurities were shown to exert great influence on the cycling life of the LiAl electrode. In order to find ways to further extend the cycling life of the LiAl electrode, a detailed study of the chemical interaction between MA and the various Li/Al intermetallic phases was performed to understand the chemical reaction involved in the course of reaction.

Cyclic voltammetry provides the most versatile electrochemical technique for studying the electrochemical formation of various Li/Al intermetallic phases at the LiAl electrode and their interaction with the solvent. The advantage of the technique is that the

reactive Li/Al intermetallic phases are formed *in situ* at the LiAl electrode surface by rapid potential scanning and their chemical reactivity towards the organic solvent can be studied immediately after formation. The above feature is particularly useful for studying the interaction of very reactive lithium rich intermetallic phases with MA. Although the information obtained from CV studies is mostly qualitative, quantitative results can also be obtained when studying the  $\alpha$ -LiAl phase with low lithium activity since the dimension of the electrode remains constant during the experiment. Thus, the thickness of the  $\alpha$ -LiAl layer can be estimated as shown in the present study.

## 2. Experimental details

### 2.1. Electrolyte and solvent

Moisture, acidic and organic impurities were removed from methyl acetate (Merck) in an elaborated procedure described in our previous paper published in this journal [17]. The purified solvent was stored at the argon-filled dry box before use.  $\text{LiClO}_4$  (BDH, dry) was ground to a fine powder and dried under vacuum at  $160^\circ\text{C}$  for 48 h. The dried salt was ground again in the argon-filled dry box before use.

### 2.2. Electrode setup and preparation

A  $\text{Ag}/\text{Ag}^+$  (0.1 M  $\text{AgNO}_3$  in acetonitrile) electrode was used as the reference electrode and a lithium wire, cut from a lithium rod (BDH, 99.9%) to the dimensions

of 30 mm length and 4 mm diameter, was used as the counter electrode. The working electrode was either an aluminium rod (Johnson Matthey, JM340) with an exposed cross-sectional area of  $0.13 \text{ cm}^2$ , or an aluminium wire (BDH, 99.9%) of 0.705 mm diameter and  $0.56 \text{ cm}^2$  working area. All working electrodes used were prepared by firstly degreasing with acetone, then mechanically polishing to a mirror finish using alumina powder, and finally cleaned by immersion in methyl acetate in an ultrasonic bath to remove water contamination. The electrode was then dried in a stream of argon before use.

### 2.3. Apparatus and measurements

All electrochemical measurements were performed using a Princeton Applied Research (PAR) 175 Universal Programmer, a PAR 173 Potentiostat/Galvanostat, and a PAR 179 Digital Coulometer/Current-to-Voltage Converter. The signal was recorded by an Esterline Angus Model 575 X-Y recorder. All the experiments were performed in a three-electrode cell put inside a dry box under argon at a slightly positive pressure above the atmospheric pressure.

Infrared spectra were taken by a Perkin-Elmer 157G Grating Infrared Spectrophotometer using sodium chloride pellet cells. NMR spectra were recorded by a Varian EM360A NMR Spectrometer. Electronic absorption spectra of freshly prepared solutions were measured by a Shimadzu UV-Visible Recording Spectrophotometer model UV-250 and the signal was recorded using a Shimadzu Graphic Printer PR-1.

## 3. Results

### 3.1. General aspects

The useful potential range for cyclic voltammetric studies of the aluminium electrode in 1 M  $\text{LiClO}_4/\text{MA}$  lay between 0.0 and  $-3.2 \text{ V}$  against the  $\text{Ag}/\text{Ag}^+$  reference electrode. The anodic end was limited by aluminium dissolution, whereas the cathodic end was marked by the deposition of lithium, forming various intermetallic compounds with the aluminium substrate. To minimise any possible electrochemical reaction prior to the deposition of lithium, the working electrode was held within the band  $-1.0$  to  $-1.2 \text{ V}$  before performing the cathodic scan.

The relationship between the electrochemical potential and the various LiAl phase composition was investigated by Rao *et al.* [18]. The incorporation of lithium into aluminium leads progressively to the formation of the  $\alpha$ ,  $\beta$ ,  $\gamma$  and  $\delta$  intermetallic phases according to the phase diagram. During the phase transition, the potential should be kept constant until the whole electrode is converted from one phase into another. This feature had been observed in using the LiAl electrode in high temperature molten salts [19], but no clear potential plateau was observed at ambient temperature, even though their presence was indicated using metallurgical techniques [18].

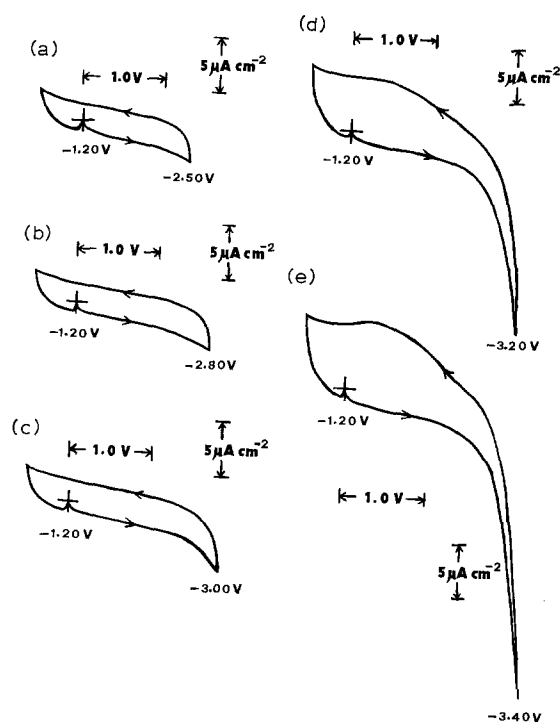


Fig. 1. The formation of the  $\alpha$ -phase on the aluminium electrode. Sweep rate:  $100 \text{ mV s}^{-1}$ .

The formation of various intermetallic LiAl compounds at room temperature was marked by a gradual change in potential [18] which reflects activity change during the incorporation of lithium into aluminium. The present work made use of the cyclic voltammetric technique to investigate the electrochemical kinetics for the formation of the above intermetallic phases at ambient temperature, as the rate of incorporation of lithium by the LiAl electrode is affected by the presence of various intermetallic phases at the electrode surface with drastic change of the lattice structure.

### 3.2. Formation of the $\alpha$ phase

The first Li/Al intermetallic phase to be formed at the aluminium electrode surface is the  $\alpha$  phase. Figure 1 shows the change in the cyclic voltammogram when the cathodic switching limits were varied from  $-2.50$  to  $-3.40 \text{ V}$  against the  $\text{Ag}^+/\text{Ag}$  electrode. The  $\alpha$  phase started to form at  $-2.50 \text{ V}$  but no corresponding typical anodic stripping peak of lithium was observed during the reverse sweep, rather, an ill-defined, very broad peak. The coulombic efficiency was low as no sweeping peak was observed in the reverse scan and the current was always smaller at the same potential during the reverse sweep than at the forward sweep. This indicated that the acceptance of lithium was lowered after the  $\alpha$  phase was formed at the electrode surface. Moreover, the formation of the  $\alpha$  phase depended on the potential and a larger deposition current was obtained at a more cathodic potential.

As the diffusion of lithium in  $\alpha$ -LiAl is slow ( $D = 10^{-10} \text{ cm}^2 \text{ s}^{-1}$  [20, 21]), the thickness of the  $\alpha$ -phase at the electrode surface is expected to be very thin and no significant change in the electrode dimension occurs

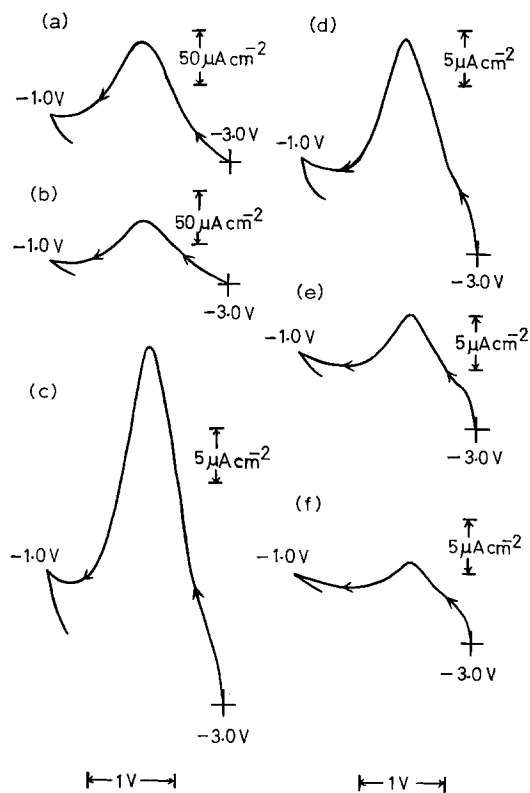


Fig. 2. Anodic stripping of electrodeposited lithium from aluminium at different sweep rates ( $\text{mV s}^{-1}$ ): (a) 50, (b) 20, (c) 10, (d) 5, (e) 2, (f) 1. Holding time at  $-3.0\text{ V}$ : 5 min.

during its formation. Thus, it could be studied by electrochemical formation at a constant potential prior to potential scan investigation. The results are shown in Fig. 2. An anodic stripping peak was clearly formed and the coulombic charge under the  $i/V$  curve for the peak was estimated to be  $190\ \mu\text{C}$ . Assuming that the electrode was totally covered by lithium atoms approximating as spheres with radius  $0.155\ \text{nm}$ ,  $26\ \mu\text{C}$  was needed to form a surface layer of lithium atoms. Thus, a given thickness of the  $\alpha$ -LiAl was indicated, which was stripped off from the electrode during the reverse sweep.

Plotting the stripping current against the scan rate, a straight line was obtained (Fig. 3). According to the following thin layer equation [22]:

$$|i_p| = n^2 F^2 |v| l A C_M^* / 2.7 RT \quad (1)$$

where  $|i_p|$  is the stripping peak currents (A),  $n$  is the number of electron transferred,  $F$  is the Faraday constant ( $\text{C mol}^{-1}$ ),  $|v|$  is the linear potential scan rate ( $\text{V s}^{-1}$ ),  $l$  is the thickness of the thin film (cm),  $A$  is the electrode area ( $\text{cm}^2$ ),  $C_M^*$  is the bulk concentration of the deposited metal in the thin film ( $\text{mol/cm}^3$ ),  $R$  is the gas constant ( $\text{J mol}^{-1} \text{K}^{-1}$ ), and  $T$  is the absolute temperature (K), the stripping currents,  $|i_p|$ , of an electrode should have a linear relationship to the scan rates,  $v$ , if the thin-layer behaviour is to be followed. The linearity of the curve shown in Fig. 3 is in good agreement with the thin-layer property of the  $\alpha$ -LiAl. Taking the concentration of lithium in the  $\alpha$  phase as 7 at/o, atom percent (i.e.  $C_M^* = 7.6 \times 10^{-3}\ \text{mol cm}^{-3}$ ),

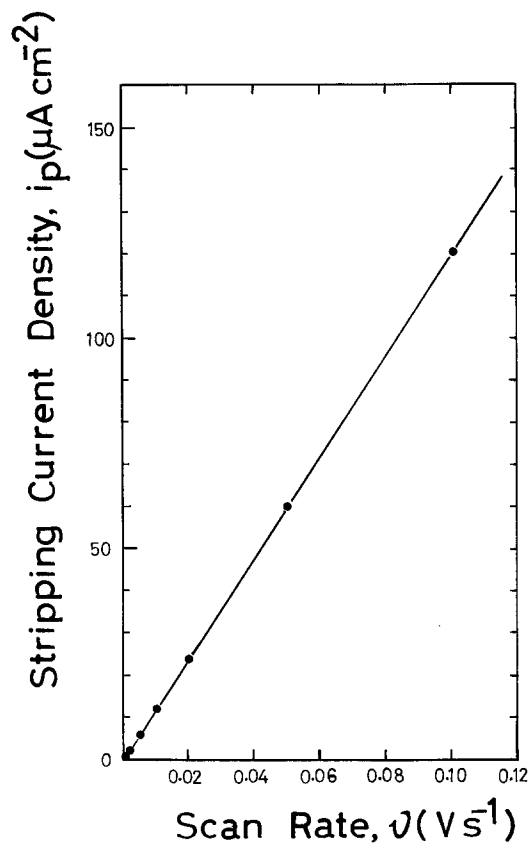


Fig. 3. A plot of stripping current density against scan rates in the  $\alpha$ -phase formation region.

the thickness of the  $\alpha$ -phase was estimated from Equation 1 to be about  $1.1\ \text{nm}$ .

### 3.3. Formation of the $\beta$ phase

Electrochemical deposition of the  $\beta$  phase was observed by further extending the cathodic potential of the electrode. The appearance of the  $\beta$  phase was marked by the occurrence of a sharp stripping peak in the voltammogram (Fig. 4). Unlike the  $\alpha$  phase, the stripping peak of the  $\beta$  phase is typical of the metal stripping peak. Two special features were observed to occur with the deposition of  $\beta$  phase at the aluminium electrode surface.

Firstly, the appearance of the stripping peak was critically dependent on the switching potential within a narrow region of  $50\ \text{mV}$  (c.f. Fig. 4a and 4b). Secondly, once the  $\beta$  phase was formed, a cross-over in the voltammogram was observed and this led to an increase in the current at the reverse sweep as compared to the forward sweep at the same potential. In other words, the nature of the electrode surface must be changed upon lithium deposition as the electrode is able to accept more lithium once the  $\beta$  phase has been formed.

Repetitive voltammetric cycling of the LiAl electrode was performed at switching potentials with either  $\alpha$  phase or  $\beta$  phase formation. The results indicated increasing stripping current upon repetitive cycling (Fig. 5) at the potential for the formation of both  $\alpha$  and  $\beta$  phases. In general, cycling led to an increase in the stripping current density in the first few cycles until

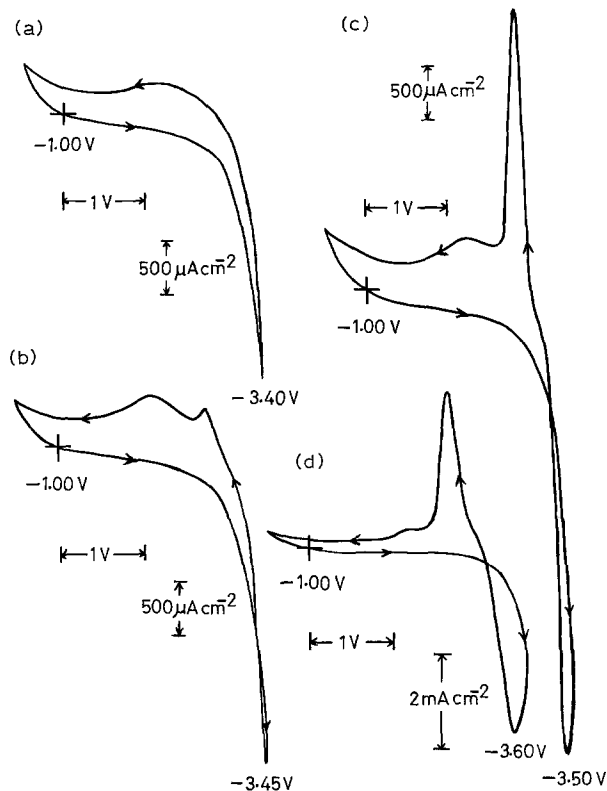


Fig. 4. The formation of the  $\beta$ -phase on the aluminium electrode. Sweep rate:  $100 \text{ mV s}^{-1}$ .

a plateau region was reached (Fig. 6). The difference in cycling with the  $\alpha$  or  $\beta$  phase was that the latter had a much larger current density compared to the former, with a magnification of nearly 160 times. Moreover, the electrode obtained after cycling was enlarged and had a rough surface with cycling of the  $\beta$  phase. This

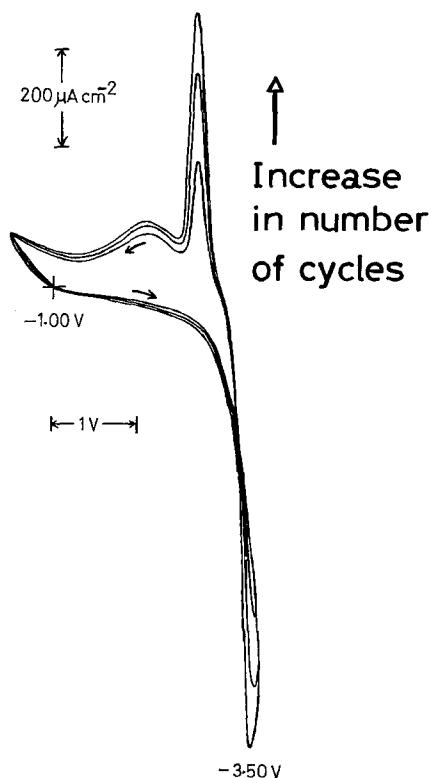


Fig. 5. The effect of cycling on the deposition and stripping of lithium from aluminium. Sweep rate:  $100 \text{ mV s}^{-1}$ .

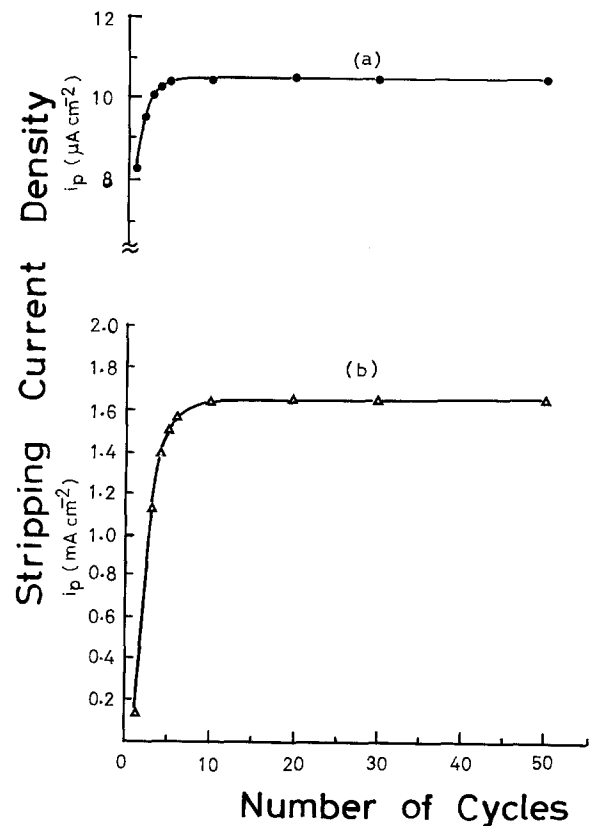


Fig. 6. The variation of stripping current density upon repetitive cycling with (a)  $\alpha$ -LiAl and (b)  $\beta$ -LiAl formation at electrode surface.

indicated that changes at both the surface and bulk of the electrode were induced by the formation of the  $\beta$  phase.

The phenomena responsible for the occurrence of a critical potential of formation, the enhancement of lithium acceptance, the development of the electrode with rough surface and enlarged electrode volume upon deposition of the  $\beta$  phase at the LiAl electrode are attributed to the difference in the lattice structure of the  $\alpha$  and  $\beta$  phases. As the atomic sizes of lithium and aluminium are similar ( $0.155 \text{ nm}$  and  $0.143 \text{ nm}$ , respectively), the initially formed  $\alpha$  phase is a solid solution of lithium in aluminium with fcc structure and  $a = 0.404 \text{ nm}$  [23–25] and thus very little change in the crystal structure of the metallic substrate was observed upon its formation. The diffusion of lithium through the  $\alpha$  phase has to be done via a vacancy mechanism. This accounts for the very small diffusion coefficient, the very small thickness of the  $\alpha$  phase layer at the electrode surface, the formation of  $\alpha$  phase over a potential range and the fact that no well defined peak is observed upon stripping.

On the other hand, the  $\beta$  phase has a bcc structure and  $a = 0.637 \text{ nm}$  [24] and thus mismatching of the crystal lattice is expected and energy is needed to inject into the system when  $\beta$  phase starts to nucleate at the  $\alpha$  phase. This accounts for the critical dependence of the  $\beta$  phase formation on the switching potential. Moreover, due to the more open structure of the  $\beta$  phase, diffusion of lithium is much quicker and this explains the enhanced acceptance of lithium once the  $\beta$  phase is formed at the electrode surface.

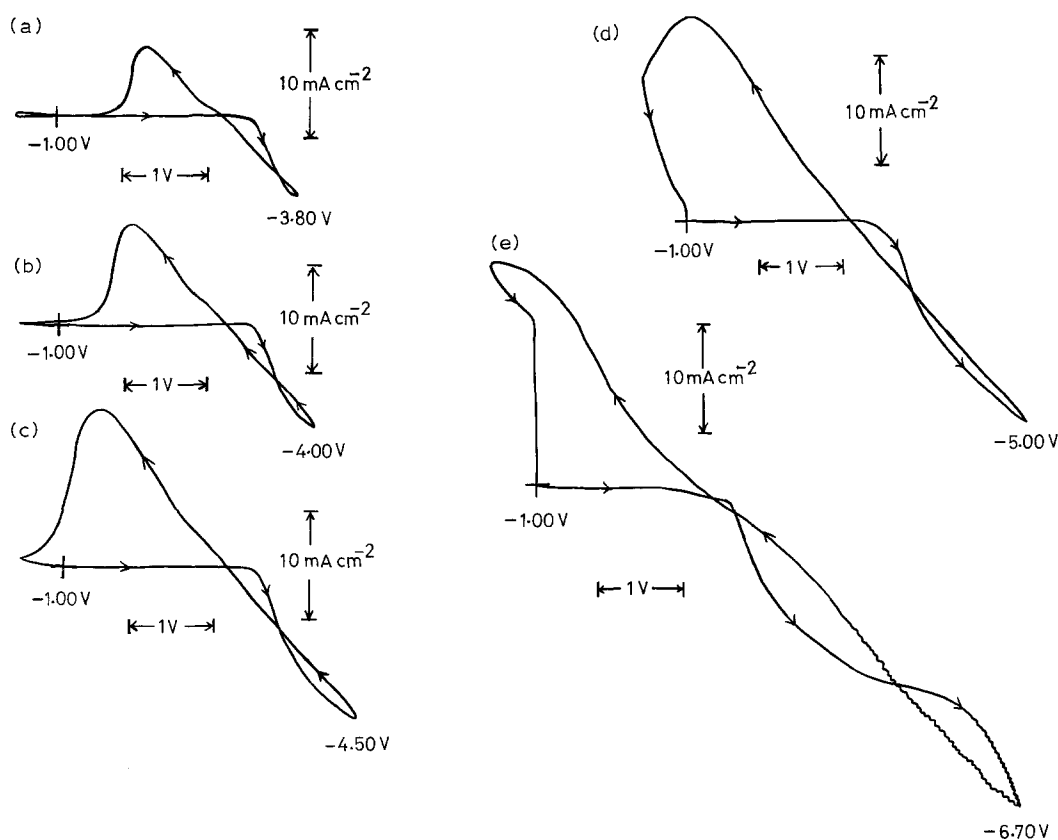


Fig. 7. The effect of switching potential on the deposition of lithium-rich Li/Al alloys. Sweep rate:  $100 \text{ mV s}^{-1}$ .

### 3.4. Formation of reactive Li/Al anode at more cathodic potentials

The formation of reactive, lithium rich, intermetallic phases at the electrode surface was studied by extending the potential more cathodically at high scan rates. The voltammograms obtained are shown in Fig. 7. In addition to having large current for deposition and stripping, three cross-over points were observed at progressively negative switching potentials. The first cross-over was due to the formation of the  $\beta$  phase and its enhancing effect on lithium acceptance, as explained in the previous section. The second cross-over occurred at a switching potential of  $-3.80 \text{ V}$  (Fig. 7a and b) and this led to current reduction upon reversing the potential. This may be due to the formation of a passivating film at the electrode surface as the result of chemical reaction between the highly reactive Li/Al alloys with the solvent. Thus, the current was smaller at the same potential in the reverse sweep as compared to the forward sweep.

However, the extension of the switching potential to  $-6.70 \text{ V}$  led to the formation of a third cross-over point (Fig. 7e). Again, the current at the reverse sweep was greater than that of the forward sweep at the same potential. However, oscillation of the current had occurred at the voltammogram and evolution of gases from the electrode surface was observed at the same time. The above facts indicated that a vigorous chemical reaction had occurred at the electrode surface and this might break down the passivated film, leading to the enhanced current during the reverse sweep.

The potentials for the occurrence of the cross-over points were highly dependent on the sweep rate. In general, the slower the sweep rate, the longer the time for the chemical reaction to occur at the electrode surface and thus less cathodic potentials were required for the appearance of the cross-over points at slow sweep rates. Fig. 8 illustrates one of the examples. Moreover, the occurrence of a large stripping current and the anodic shift in the stripping peak using slower scan rate masks the observation of the small  $\alpha$  peaks at  $-2.2 \text{ V}$  (Fig. 8a c.f. Fig. 4d).

### 3.5. Chemical reaction between the lithium electrode and methyl acetate

The chemical reaction of the solvent with the lithium electrode was studied by cycling between two lithium electrodes in  $1 \text{ M LiClO}_4/\text{MA}$  at a current density of about  $10 \text{ mA cm}^{-2}$  over an extended period of time. The solution obtained was firstly neutralized with dilute HCl, then extracted with ether and finally evaporated away the solvent to obtain the decomposition product. I.r. and n.m.r. spectra of the product were taken and compared with the spectral library. Both spectra showed excellent matching with the standard spectra of methyl acetoacetate [26].

To indicate the presence of methyl acetoacetate in the solution and to study its electrochemical property, a cyclic voltammogram and u.v. spectra of the decomposed solution, blank and solution with standard methyl acetoacetate were taken. The results are shown in Figs 9 and 10. The u.v. results clearly

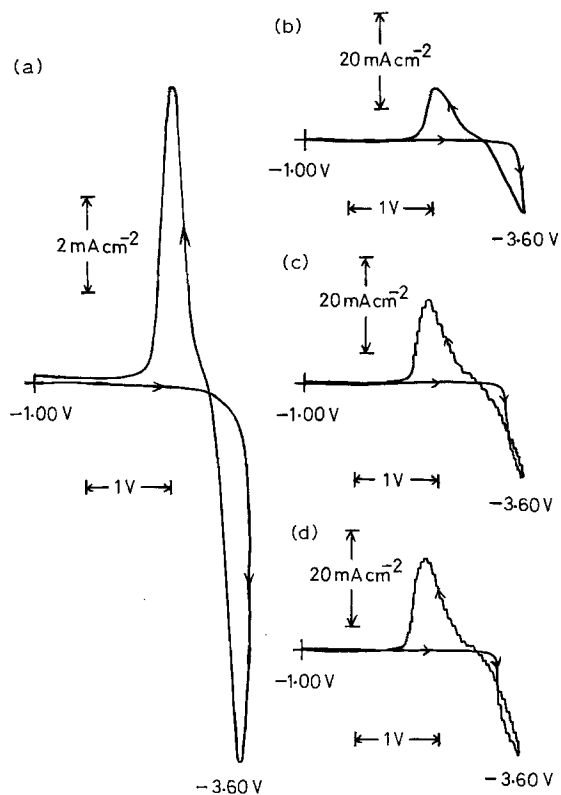


Fig. 8. The effect of sweep rate on the formation of the  $\beta$  phase. Sweep rate ( $\text{mV s}^{-1}$ ): (a) 50, (b) 20, (c) 10, (d) 5.

indicated the presence of methyl acetoacetate in the solution and the electrochemical experiments showed that methyl acetoacetate was reduced at  $-2.8$  V with no corresponding anodic peak. Thus, it involved an irreversible electron transfer reaction and accumulation of impurities would occur once they had reacted at the electrode surface.

In summary, both the electrochemical and u.v. results supported the fact that methyl acetoacetate was the major decomposition product between lithium and methyl acetate. One possible reaction mechanism for the above decomposition reaction is postulated as follows

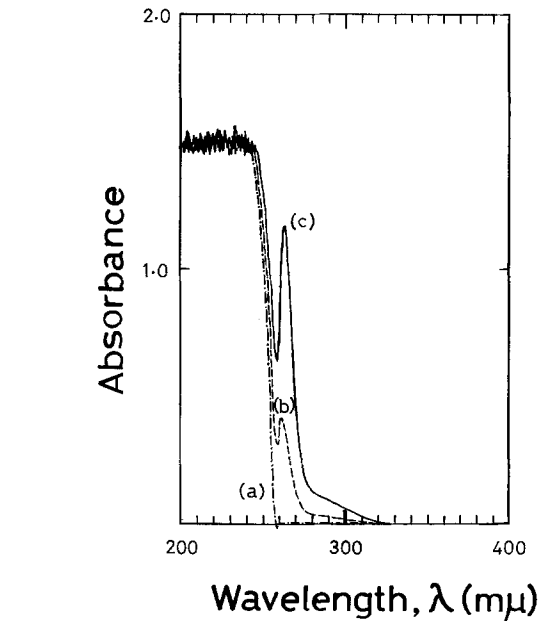


Fig. 10. Absorption spectra for methyl acetoacetate and the electrochemical decomposition product of methyl acetate: (a) methyl acetate solution blank, (b) addition of  $10 \mu\text{L}$  electrochemical decomposition product of methyl acetate to solution (a) above ( $3.5 \text{ mL}$ ), (c) addition of  $1 \mu\text{L}$  methyl acetoacetate to solution (b) above ( $3.5 \text{ mL}$ ).

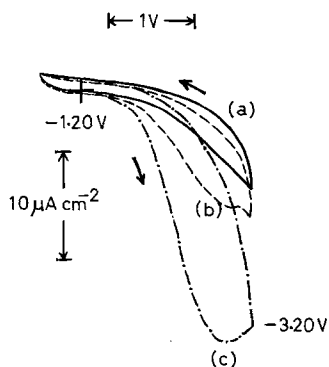
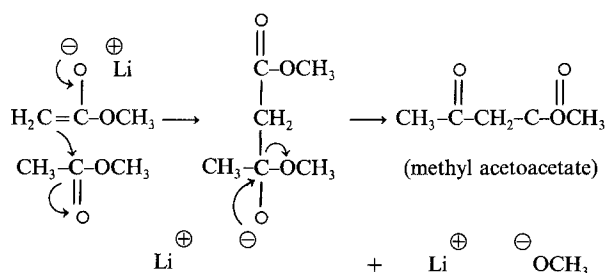
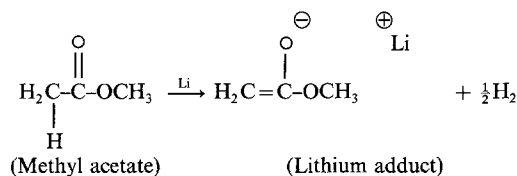


Fig. 9. The cyclic voltammograms for methyl acetoacetate and the decomposition product of methyl acetate. Sweep rate:  $100 \text{ mV s}^{-1}$ . (a)  $1 \text{ M LiClO}_4/\text{MA}$  before decomposition, (b)  $1 \text{ M LiClO}_4/\text{MA}$  after electrochemically decomposed at  $-6.70 \text{ V}$  against  $\text{Ag}/\text{Ag}^+$  reference electrode, (c) addition of  $50 \mu\text{L}$  methyl acetoacetate to solution (b) above ( $10 \text{ mL}$ ).

#### 4. Conclusions

The following conclusions can be drawn from the work performed.

1. Cyclic voltammetry was shown to be a promising method for studying the formation of the very reactive  $\text{Li}/\text{Al}$  electrode *in situ* at the electrode surface.

2. The formation of  $\alpha$ ,  $\beta$  and other lithium rich intermetallic phases at the electrode surface at ambient temperature was shown to have a strong effect on the electrode kinetics of the  $\text{Li}/\text{Al}$  electrode.

3. The formation of the  $\alpha$  phase at the  $\text{Li}/\text{Al}$  electrode led to decreased lithium acceptance upon reversing the potential and with no clear lithium stripping peak in the voltammogram. The thickness of the  $\alpha$  phase layer at the electrode surface was found to be about  $1.1 \text{ nm}$  using the hold and sweep method.

4. The deposition of the  $\beta$  phase on the LiAl electrode depended critically on the potential and its formation led to increased acceptance of lithium, roughening of the electrode surface and enlargement of the bulk of the electrode. The effect of the  $\beta$  phase is attributed to the difference in the lattice structure of the  $\beta$  phase as compared to the  $\alpha$  phase.

5. The formation of highly reactive Li/Al alloys at more cathodic potential was shown to lead to the formation of a passivating film at  $-3.80$  V, which could be broken down at more cathodic potentials when the electrode surface had undergone vigorous chemical reaction with the solvent.

6. Methyl acetoacetate was identified to be the major decomposition product in chemical reaction occurring between methyl acetate and the lithium electrode. A possible reaction mechanism was proposed.

#### Acknowledgement

We thank the Hong Kong University and UPGC Research Grant Committee for their continued support for the lithium battery project.

#### References

- [1] V. R. Koch and S. B. Brummer, *Electrochim. Acta* **23** (1978) 55.
- [2] R. D. Rauh, T. F. Reise and S. B. Brummer, *J. Electrochem. Soc.* **125** (1978) 186.
- [3] R. D. Rauh and S. B. Brummer, *Electrochim. Acta* **22** (1977) 75.
- [4] R. Selim and P. Bro, *J. Electrochem. Soc.* **121** (1974) 1457.
- [5] S. G. Meibuhr, *ibid.* **117** (1970) 56.
- [6] S. I. Tobishima and T. Okada, *J. Appl. Electrochem.* **15** (1985) 317.
- [7] G. H. Newman, R. W. Francis, L. H. Gaines and B. M. L. Rao, *J. Electrochem. Soc.* **127** (1980) 2025.
- [8] T. R. Jow and C. C. Liang, *ibid.* **129** (1982) 1429.
- [9] A. N. Dey and E. J. Rudd, *ibid.* **121** (1974) 1294.
- [10] V. R. Koch, *ibid.* **126** (1979) 181.
- [11] V. R. Koch and J. H. Young, *ibid.* **125** (1978) 1371.
- [12] J. L. Goldman, R. M. Mank, J. H. Young and V. R. Koch, *ibid.* **127** (1980) 1461.
- [13] P. G. Glugla, *ibid.* **130** (1983) 113.
- [14] R. D. Rauh and S. B. Brummer, *Electrochim. Acta* **22** (1977) 85.
- [15] F. W. Dampier and S. B. Brummer, *ibid.* **22** (1977) 1339.
- [16] J. S. Fooks and J. McVeigh, *J. Electrochem. Soc.* **130** (1983) 628.
- [17] Y. S. Fung and H. C. Lai, *J. Appl. Electrochem.* **19** (1989) 239.
- [18] B. M. L. Rao, R. W. Francis and H. A. Christopher, *J. Electrochem. Soc.* **124** (1977) 1490.
- [19] Y. S. Fung, D. Inman and S. H. White, *J. Appl. Electrochem.* **12** (1982) 669.
- [20] C. A. Melendres, *J. Electrochem. Soc.* **124** (1977) 650.
- [21] L. P. Costas and E. C. Hoxie, *U.S. Atomic Energy Comm. NMI-4997* (1964) pp. 26-35.
- [22] A. J. Bard and L. R. Faulkner, 'Electrochemical Methods—Fundamental and Applications', John Wiley & Sons, New York (1980).
- [23] R. P. Elliott, 'Constitution of Binary Alloys', 1st supplement, McGraw-Hill, New York (1965) p.42.
- [24] M. Hansen, 'Constitution of Binary Alloys', McGraw-Hill, New York (1958), pp. 104-5.
- [25] F. A. Shunk, 'Constitution of Binary Alloys', 2nd supplement, McGraw-Hill, New York (1969) pp. 27-8.
- [26] H. C. Lai, Electrochemical Studies of the Lithium-Aluminium Anode in Methyl Acetate, M. Phil. Thesis, University of Hong Kong (1986).